Electronic Supplementary Material (ESI) for ChemComm.

Supporting Information

Stretchable, Transparent and Imperceptible Supercapacitors Based on Au@MnO_2 Nanomesh Electrodes

Junlong Yang[1, 2], Tianzeng Hong[1], Jue Deng[3], Yan Wang[1], Fan Lei[1], Jianming Zhang[1, 4], Bo Yu[5] Zhigang Wu[6], Xinzheng Zhang[2], Chuan Fei Guo[1, *]

[1]Department of Materials Science and Engineering & Shenzhen Engineering Research Center for Novel Electronic Information Materials and Devices, Southern University of Science and Technology, Shenzhen 518055, China

[2]School of Physics and TEDA Institute of Applied Physics, Nankai University, Tianjin, China

[3]Department of Mechanical Engineering Massachusetts Institute of Technology, Cambridge, MA 02139, USA

[4]Academy for Advanced Interdisciplinary Studies, Southern University of Science and Technology, Shenzhen, China

[5]Ningbo Fengcheng Advanced Energy Materials Research Institute, Ningbo, Zhejiang, 315500, China

[6]State Key Laboratory of Digital Manufacturing Equipment and Technology, Huazhong University of Science and Technology, Wuhan, China

*To whom correspondence should be addressed. Email: guocf@sustc.edu.cn

Experimental Details

Preparation of Au@MnO₂ Nanomesh: The Au nanomesh was fabricated by using our reported method called grain boundary lithography, [1] and then transferred onto the PDMS substrate. The thickness of prepared Au nanomesh is ≈ 40 nm. The Au@MnO_2 nanomesh film was prepared by electrodeposition over Au nanomesh. Typically, the Au nanomesh films were immersed into the plating solution containing 50×10^{-3} $_{\mathrm{M}}$ Na_2SO_4 aqueous solution and 1×10^{-3} $_{\mathrm{M}}$ $Mn(Ac)_2$ aqueous solution using potential of 0.75 V vs SCE and Pt as reference electrode. Afterwards, the obtained Au@MnO_2 nanomesh film was washed by DI water and dried using nitrogen gas gun. The loading of MnO_2 was varied with different quantity of electricity per unit area of electrode, including 0.004 C/cm^2, 0.008 C/cm^2, 0.016 C/cm^2. The deposition time is about 30 s for 1 cm^2 electrode using quantity of electricity density of 0.008 C/cm^2.

The Thickness Calculation of MnO_2 Layer: Based on the quantity of electricity and the chemical reaction of MnO_2 during electro-deposition as shown below:

$$(Mn^{2+}) + 2H_2O —— MnO_2 + (4H^+) + (2e\text{-})$$

the mass of deposited MnO_2 should be following the equation below:

$$m = (Q/2F) * M_r$$

for which Q is the quantity of electricity used during deposition, F is Faraday's constant, 96500 C/mol, and M_r is the relative molecular mass, 87 for MnO_2. We assume that the area of Au nanomesh is 1 cm^2 and the MnO_2 flake is a complete layer. Thus, the Q is 0.008C, the calculated mass of MnO_2 is 3.6 μg and the thickness is about 7.2 nm using the density of 5.3 g/cm^3 for MnO_2. It should be noted that the electrode is a mesh structure, and the MnO_2 grow along with Au skeleton during deposition, which should form a thin layer with mesh structure instead of a complete MnO_2 layer. Therefore, the calculated thickness of 7.2 nm for MnO_2 is not rigorous and only for reference when considering the mesh structure. We only give the areal capacitance and energy density in this work to keep the data rigorous.

Preparation of the Transparent Stretchable Planar Supercapacitor (TSPS) Device: 1 g of PVA, 10g of H_2O and 0.2 g Na_2SO_4 were mixed and heated up to 95°C under vigorous stirring. After 1 h stirring and cooling down to the ambient temperature, PVA/Na_2SO_4 gel electrolyte was obtained.

For the highly transparent supercapacitor, the interdigital electrodes of Au@MnO_2 nanomesh was achieved using a needle scratching on the surface flowing an interdigital template. The gap between two fingers is about 50 μm, and the width of the finger is about 600 μm. The transparent stretchable planar supercapacitor (TSPS) device was produced by placing the gel electrolyte on the interdigital electrodes of Au@MnO_2 nanomesh and packaged with transparent plastic wrap.

Materials Characterization: Transmittance measurement was carried out using UV−vis spectrophotometer (PerkinElmer Model Lambda 950). The water contact angle was determined after a water droplet of 1 μL placed on the surface of test sample via an optical video contact angle instrument (VCA Optima XE, AST) at room temperature. The morphologies of the Au nanomesh and Au@MnO_2 nanomesh were measured using a scanning electron microscope (MIRA3, TESCAN) and transmission electron microscopy (FEI Tecnai F30). Electrochemical performance of Au@MnO_2 nanomesh was measured using Electrochemical Station (CS350H, Wuhan CorrTest). The stretchability and mechanical durability of the TSPS device was evaluated using a step motor (WS150-100).

Electrochemical Performance Characterization: The electrochemical performance of the Au@MnO_2 nanomesh electrode and TSPS device were investigated by cyclic voltammograms (CV) and galvanostatic charge-discharge (GCD) cycling using an electrochemical workstation (CS350H, Wuhan CorrTest Instruments). 0.1 $_M$ Na_2SO_4 aqueous solution was used as the electrolyte for Au@MnO_2 nanomesh electrode in three-electrode system. PVA/Na_2SO_4 gel was employed as the solid-state electrolyte for TSPS device in two-electrode system. The areal capacitance of the electrode or device was calculated according to the following equation:

$$C = 2i/[A(\Delta V/\Delta t)]$$

where i is the applied current, A is the area of electrode, ΔV/Δt is the slope of the discharge curves after the IR drop.

Energy Density Calculation: The energy density and powder density of the TSPS device are following the equation:

$$E = \left({}^{1}\!/_{2} \times C \times (\Delta V)^2\right)/3600$$

$$P = (E/\Delta t) \times 3600$$

which E is the areal energy density (Wh/cm^2), C is the areal capacitance (F/cm^2), ΔV is the discharge voltage range (V), P is the power density (W/cm^2), and Δt is the discharge time (s). According to Figure 2 in the Manuscript, the areal capacitance is 530 F/cm^2 at a current density of 0.0125 mA/cm^2, the discharge voltage range is 0.8 V, and the discharge time is 78.2s. Thus, the calculated energy density of TSPS device is 0.047 μWh/cm^2 at power density of 2.16 μW/cm^2.

Supporting Figures.

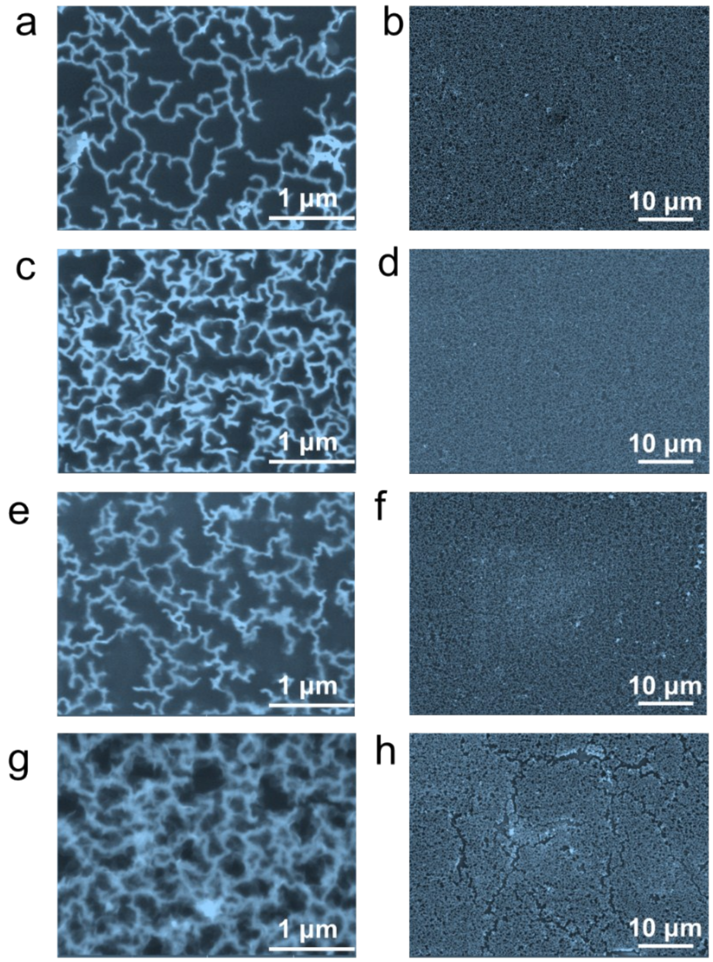

Figure S1. The SEM images of Au nanomesh a) and b), and Au nanomesh after MnO_2 electro-deposition with different charge quantity. c) and d) 0.004 C/cm^2, e) and f) 0.008 C/cm^2, g and h) 0.016 C/cm^2. The MnO_2 layer was electro-deposited on the Au nanomesh, forming a-few-nanometer-thick flakes. And the thickness of MnO_2 layer is up to the electro-deposited charge quantity, the higher the charge quantity used, the thicker the MnO_2 layer is. Such thicker MnO_2 layer results in the unclear images visually that make the image looks haze, while it should be the increased mas of deposited MnO_2 layer that evidenced from TEM image in Figure 1e in manuscript.

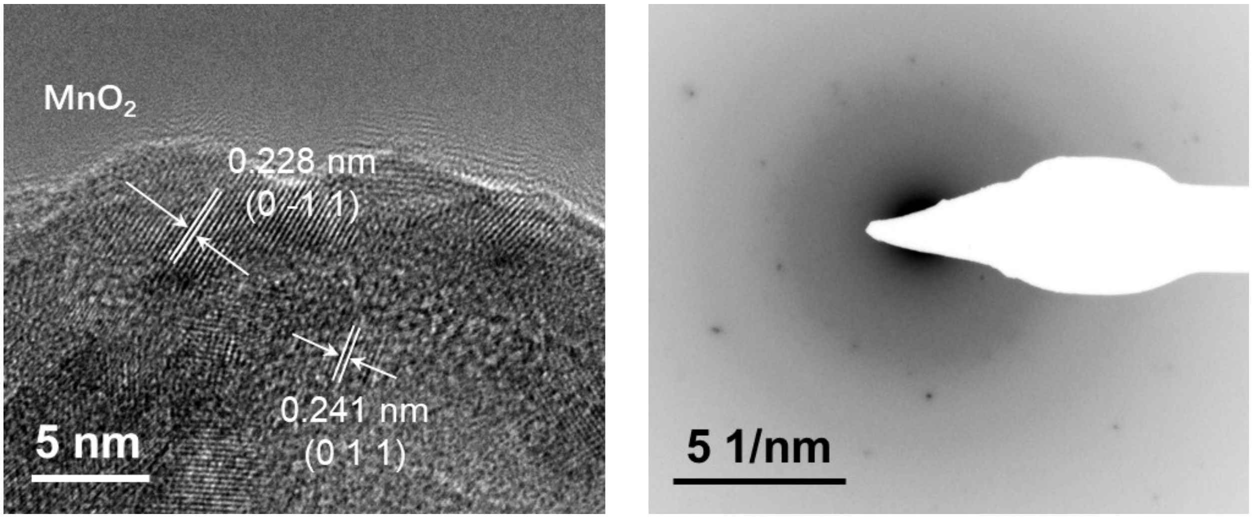

Figure S2. The high resolution TEM image (left) and corresponding SAED patterns (right) of MnO_2 nanosheets coated on Au core after electro-deposition. The d-spacing sequences for the MnO_2 flakes are 0.241, 0.228, and 0.152 nm, which are indexed to be the interlayer spacing of (0 1 1), (0 -1 1) and (0 1 4) planes (Referred to the ICCD card no.01-72-6745).

Figure S3. Photographs of water droplet on Au nanomesh and the Au@MnO2 nanomesh, using PDMS as the substrate.

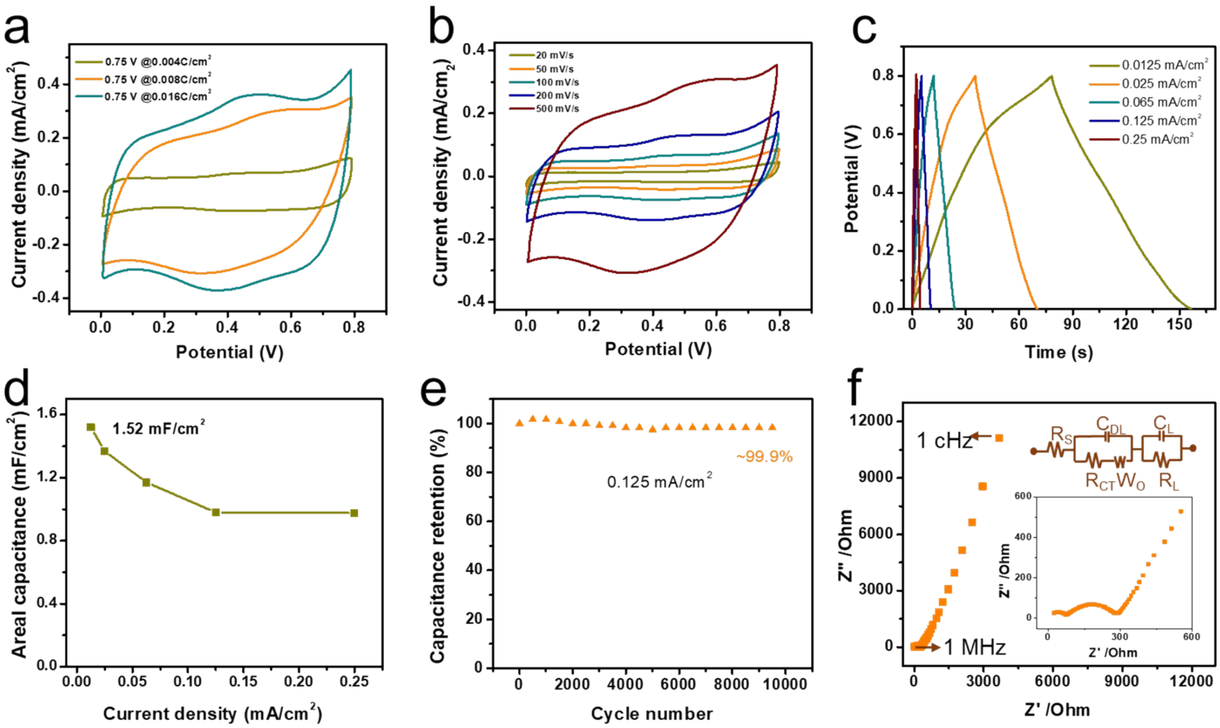

Figure S4. a) CV curves of Au@MnO_2 nanomesh with different MnO_2 loading at electro-deposition voltage of 0.75V, scan rate at 500 mV/s. b) CV curves of the Au@MnO_2 nanomesh (0.008 C/cm^2) at different scan rates. c) and d) Galvanostatic CD curves and dependence areal capacitance of the Au@MnO_2 nanomesh (0.008 C/cm^2) at different current density. e) Nyquist impedance plot of the Au@MnO_2 nanomesh (0.008 C/cm^2) supercapacitor. f) Nyquist plot of the Au@MnO_2 nanomesh electrode and fitted equivalent circuit (insets). R_S is the series resistance, C_{DL} is the double-layer capacitance, R_{CT} is the charge transfer resistance, W_O is the Warburg impedance, C_L denotes the pseudo capacitance, and R_L is the leakage resistance.

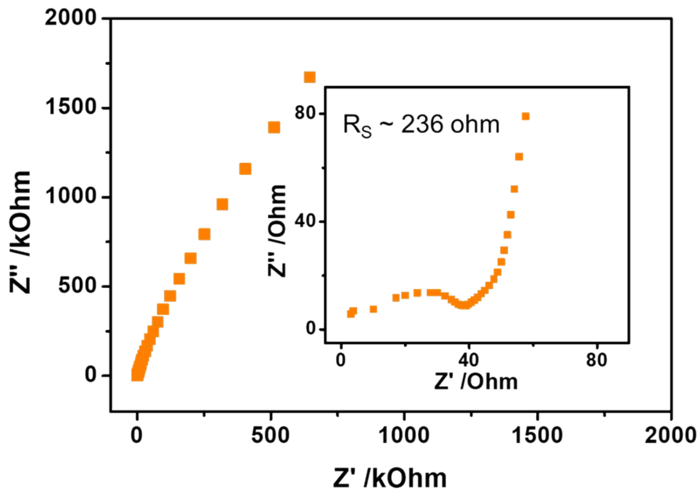

Figure S5. The Nyquist plot of the Au nanomesh electrode and fitted equivalent circuit (insets), the Rs is about 236 Ohms.

Note:

The electrochemical performance of the Au@MnO_2 nanomesh was evaluated through cyclic voltammetry (CV) and galvanostatic charge–discharge (GCD) measurements in three-electrode configuration in 1 M Na_2SO_4 solution. As shown in **Figure S4**a, the CV curves of the Au@MnO_2 nanomesh with different MnO_2 loading exhibit near symmetrical rectangular shapes at a scan rate of 500 mV/s, suggesting ideal capacitive behavior. The areal current density values are increased in higher loadings of MnO_2. Whereas the Au nanomesh core tended to fail by forming cracks with the presence of higher loading of MnO_2, as seen from the SEM images (**Figure S1**). The higher loading also leads to undesired lower transparency. Thus, 0.008 C/cm^2 was selected as the terminal condition for electrodepositing to deposit proper thickness of MnO_2 on the Au nanomesh electrodes. The CV curves for Au@MnO_2 nanomesh was measured at various scan rates from 20 to 500 mV/s (**Figure S4**b), showing a nearly rectangular-shaped curves even at high scan rates. Such CV curves revealed excellent capacitive behavior of the Au@MnO_2 nanomesh electrode, which is mainly attributed to the fast charge propagation between MnO_2 and highly conducting Au core due to the strong coupling interaction [2]. **Figure S4**c shows galvanostatic charge–discharge (GCD) curves of the Au@MnO_2 nanomesh at a potential window from 0 to 0.8 V with corresponding current densities from 0.0125 to 0.25 mA/cm^2. The GCD curves exhibit nearly triangular shape, indicating the formation of the electrochemical double layer and efficient charge propagation.

The areal capacitance with various current densities were calculated from the discharging slope after the ohmic potential (IR) drop and is shown in **Figure S4d**. The areal capacitance of the Au@MnO_2 nanomesh is 1.52 mF/cm^2 at 0.0125 mA/cm^2 current density, and remains 64% of the areal capacitance as the current density increases 0.25 mA/cm^2. Moreover, **Figure S4e** reveal that the areal capacitance preserves about 98% after 10,000 GCD cycles at a current density of 0.125 mA/cm^2, exhibiting excellent long-term stability of the Au@MnO_2 nanomesh. We also investigated the electrochemical impedance spectroscopy of the Au@MnO_2 nanomesh to understand the fundamental behavior at the electrode–electrolyte interface. The Nyquist impedance plot of Au@MnO_2 nanomesh in the frequency range of 10^{-2} to 10^6 Hz was shown in **Figure S4f**, and fitted equivalent circuit was also given in the inset. Based on the nearly vertical shape at low frequencies, the estimated series resistance (R_S) of Au nanomesh is figured out to be 236 Ω and R_S of Au@MnO2 nanomesh (**Figure S5**) is 408 Ω, which is higher than that of Au nanomesh. It should be attribute to the more complete structure of Au nanomesh. However, the series resistance still remains the high conductivity, which attributed to the high conductivity of Au nanomesh and strong interaction between MnO_2 and the Au core.

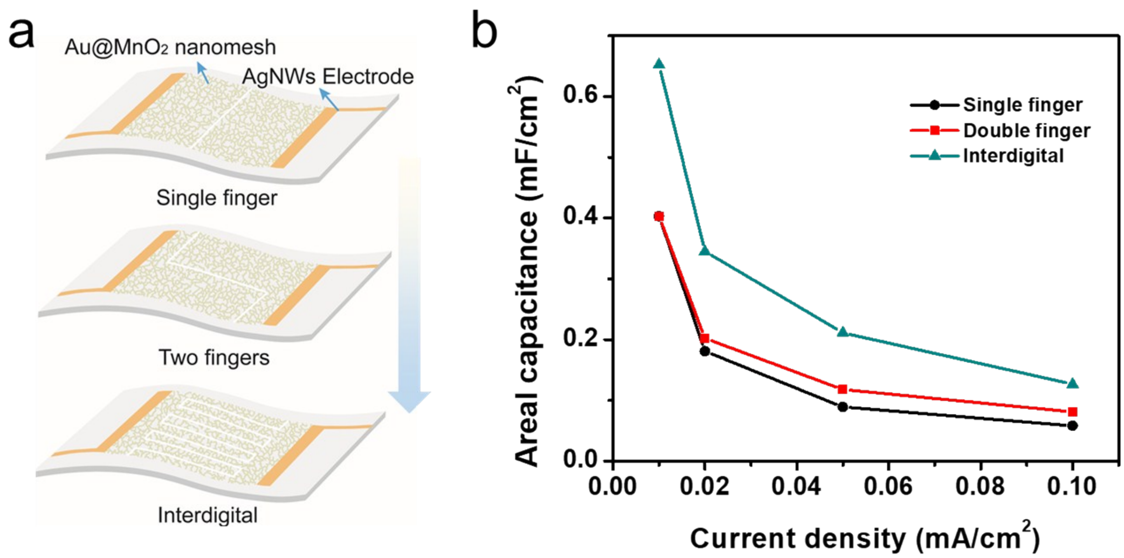

Figure S6. a) Schematic illustration of the transparent planar supercapacitor based on Au@MnO_2 nanomesh electrodes with different number of fingers. b) The areal capacitance of three transparent planar supercapacitor devices based on Au@MnO_2 nanomesh electrodes with different fingers.

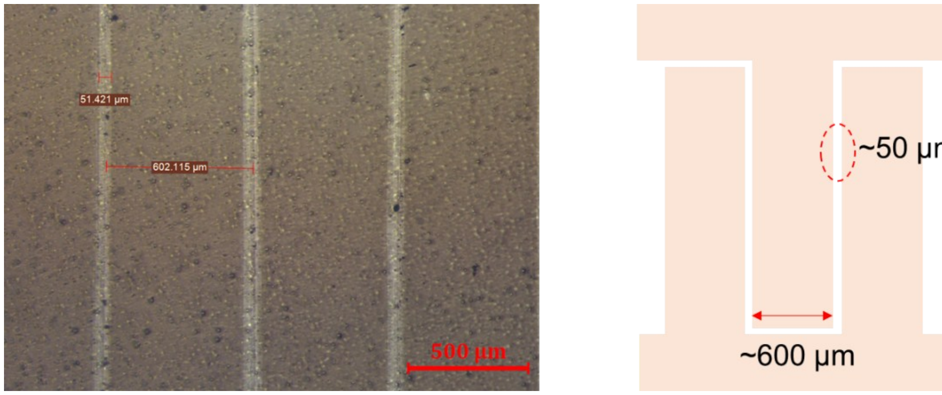

Figure S7. The optical image and schematic illustration of Au@MnO_2 nanomesh electrodes, the gap between two fingers is about 50 µm, and the width of finger is about 600 µm.

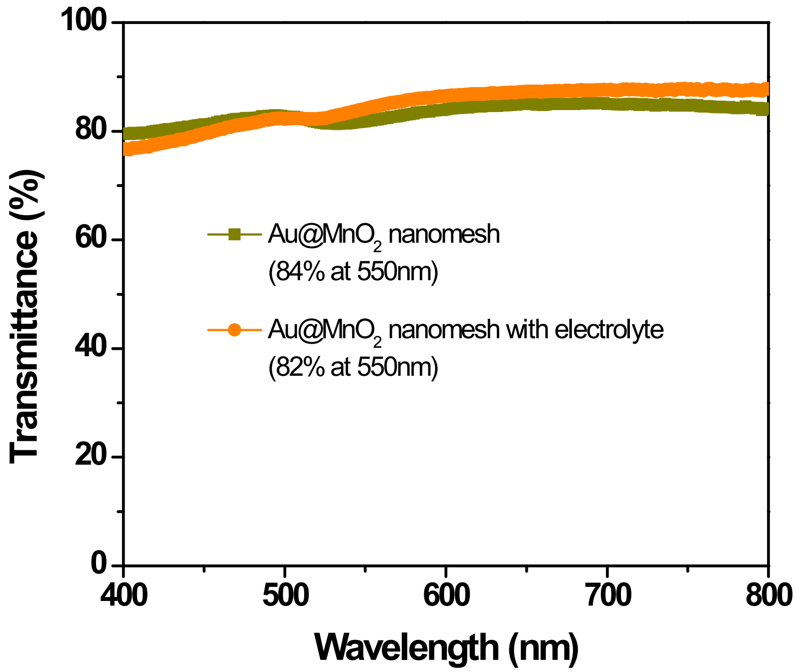

Figure S8. The optical performance of Au@MnO_2 nanomesh and the transparent stretchable planar supercapacitor (TSPS) device using PVA/Na_2SO_4 as solid-state electrolyte.

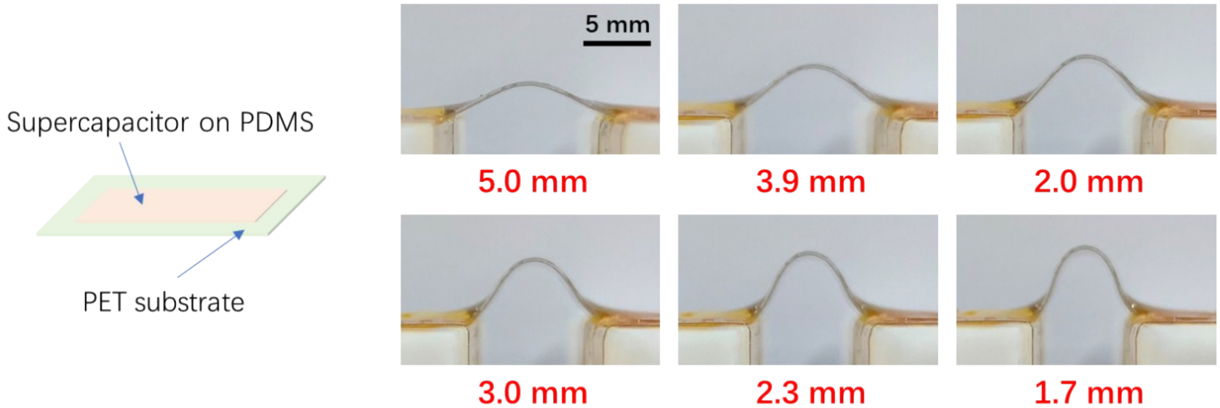

Figure S9. Schematic illustration of the device for bending tests and the digital photos of the device under different bending radii.

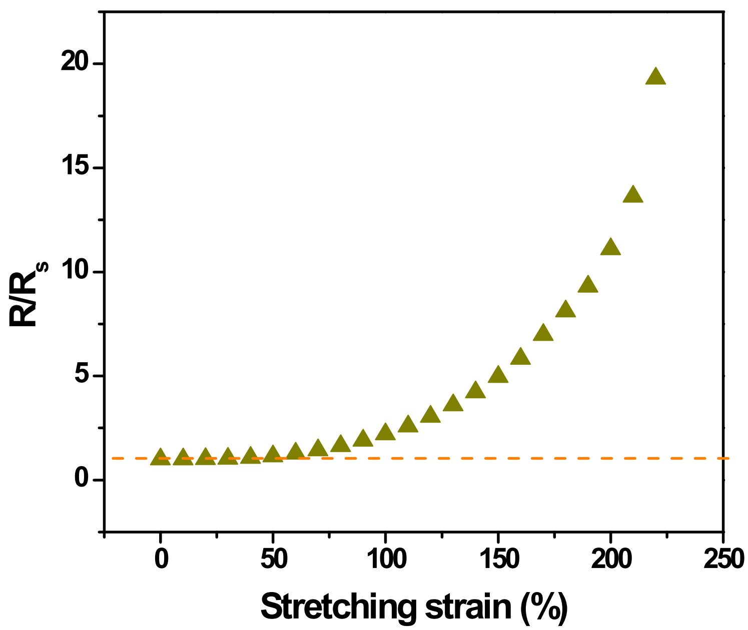

Figure S10. The resistance change of Au nanomesh electrode under different stretching strain, Rs represents the resistance under stretching.

Table. S1 Performance of transparent and flexible supercapacitors based on different electrodes and active materials.

Electrodes/Active Materials (Thickness, structure)	Transmittance @550 nm (%) of device or electrode	Areal Capacitance of device (C, μF/cm^2)	Maximal Strain (%)	C/C_0, %, at maximal strain	Ref.
Ag-Au-Ppy (~ 45 nm, network)	65, device	580 at 5.8 μA/cm^2	50	~100%	[3]
Ag-Au (~ 35 nm, network)	85, electrode	210 at 10 μA/cm^2	60	90	[4]
Au nanowire (2 nm, network)	79, electrode	56.7 at 0.25 A/g	30	95	[5]
Graphene (3.4 nm, sheet)	57, device	5.8 at 0.8 μA/cm^2	40	~100	[6]
Au nanowire (~1 μm, network)	55, device	176 at 3.3 mA/cm^2	100	76	[7]
CNT-MnO_2 (/, network)	/	157 at 2 mA/cm^2	100	~100	[8]
PEDOT:PSS/AgNFs (~90 nm, film)	77.4, device	910 at 5 mV/cm^2	/	/	[9]
Au-MnO_2 (/, network)	63, device	660 at 2.5 μA/cm^2	/	/	[10]
Au-MnO_2 (~53 nm, mesh)	36, device	795 at 5 μA/cm^2	/	/	[2]
Au@MnO_2 nanomesh (~47 nm, nanomesh)	82.1, device	530, device at 12.5 μA/cm^2	160	79	This work

Reference

1. Guo, C.F., T. Sun, Q. Liu, Z. Suo, and Z. Ren, *Nat. Commun.*, 2014. 5: p. 3121.
2. Qiu, T., B. Luo, M. Giersig, E.M. Akinoglu, L. Hao, X. Wang, L. Shi, M. Jin, and L. Zhi, *Small*, 2014. 10(20): p. 4136-4141.

3. Moon, H., H. Lee, J. Kwon, Y.D. Suh, D.K. Kim, I. Ha, J. Yeo, S. Hong, and S.H. Ko, *Sci. Rep.*, 2017. 7: p. 41981.
4. Lee, H., S. Hong, J. Lee, Y.D. Suh, J. Kwon, H. Moon, H. Kim, J. Yeo, and S.H. Ko, *ACS Appl. Mat. Interfaces*, 2016. 8(24): p. 15449-15458.
5. Gong, S., Y. Zhao, Q. Shi, Y. Wang, L.W. Yap, and W. Cheng, *Electroanalysis*, 2016. 28(6): p. 1298-1304.
6. Chen, T., Y. Xue, A.K. Roy, and L. Dai, *Acs Nano*, 2013. 8(1): p. 1039-1046.
7. Wang, Y., S. Gong, D. Dong, Y. Zhao, L.W. Yap, Q. Shi, T. An, Y. Ling, G.P. Simon, and W. Cheng, *Nanoscale*, 2018. 10(34): p. 15948-15955.
8. Xu, P., B. Wei, Z. Cao, J. Zheng, K. Gong, F. Li, J. Yu, Q. Li, W. Lu, and J.-H. Byun, *ACS nano*, 2015. 9(6): p. 6088-6096.
9. Singh, S.B., T. Kshetri, T.I. Singh, N.H. Kim, and J.H. Lee, *Chem. Eng. J.*, 2019. 359: p. 197-207.
10. Kiruthika, S., C. Sow, and G. Kulkarni, *small*, 2017. 13(40): p. 1701906.